




Spectral properties of a Co-decorated quasi-two-dimensional GaSe layer

Ireneusz Weymann ^{1,*} Maciej Zwierzycki ^{2,†} and Stefan Krompiewski ²

¹*Faculty of Physics, Adam Mickiewicz University, 61-614 Poznań, Poland*

²*Institute of Molecular Physics, Polish Academy of Sciences, 60-179 Poznań, Poland*



(Received 1 April 2020; revised 10 August 2020; accepted 11 August 2020; published 21 August 2020)

Based on reliable *ab initio* computations and the numerical renormalization group method, systematic studies on a two-dimensional GaSe monolayer with Co adatoms have been carried out. It is shown that the stable lowest-energy configuration of the system involves the Co adatom located over a Ga atom. For such a configuration, it is demonstrated that the electronic and magnetic properties of the system can be effectively controlled by means of external factors, such as magnetic field, gate voltage, or temperature. Moreover, if properly tuned, the GaSe-Co system can also exhibit the Kondo effect. The development of the Kondo phenomenon is revealed in the local density of states of the Co adatom, its magnetic field dependence, which presents the splitting of the Kondo peak, as well as in the temperature dependence of the conductance, which exhibits scaling typical of the spin- $\frac{1}{2}$ Kondo effect.

DOI: [10.1103/PhysRevB.102.075309](https://doi.org/10.1103/PhysRevB.102.075309)

I. INTRODUCTION

Two-dimensional (2D) and quasi-two-dimensional monolayers have been recently intensively studied, both experimentally and theoretically, because they exhibit many remarkable physical phenomena, including mechanical, optoelectronic, electric, and magnetic ones [1–6]. Moreover, it is now also well known that such systems can be additionally functionalized in various ways, e.g., by chemical doping [7], and by introducing either adatoms or vacancies and other defects [8–10]. In fact, the presence of magnetic adatoms can give rise to interesting strongly correlated phenomena, such as the Kondo effect [11,12], which, despite the fact that a few decades have passed since its first observation in artificial atoms [13], still attracts considerable attention [14–16]. Quite interestingly, the spectral signatures of adatoms placed on 2D materials have been analyzed in the Kondo regime in a number of works [17–22]. However, given a variety of 2D and quasi-2D materials, there are still some aspects that need to be explored.

The system under consideration here is the GaSe monolayer with a unit cell composed of a Ga-Ga dimer covalently bonded to six Se atoms [7,23]. Similar to many other low-dimensional graphenelike layers, this material is also an object of particular interest. This is especially so because, in contrast to graphene, GaSe is a semiconductor with a pronounced energy gap—and can therefore serve as a transistor and possibly also as a promising material for solar energy harvesting [24]. In this paper we in particular focus on examining the spectral properties of a GaSe monolayer decorated with Co adatoms. The analysis is performed by combining first-principles calculations with the nonperturbative numerical renormalization

group (NRG) method [25]. The *ab initio* computations are used to determine the energetically most favorable system's configuration, the density of states as well as the electron occupation and magnetic moment of the Co adatom. Then, the spectral properties of the adatom are determined by using NRG for an effective Anderson-like Hamiltonian. It is shown that the electronic and magnetic properties of the system can be tuned by external means, such as temperature, magnetic field, or gate voltage. Furthermore, it is also demonstrated that the GaSe-Co system can exhibit the Kondo effect, if appropriately tuned.

We believe that the accurate results and predictions presented in this paper shall foster further experimental investigations on 2D materials decorated with magnetic adatoms. In particular, our results suggest that the GaSe system, when decorated with Co adatoms, can reveal interesting properties, such as a gate-voltage-controlled enhanced conductance due to the Kondo effect, which may be attractive for future applications in electronics and spintronics.

II. ELECTRONIC STRUCTURE AND EFFECTIVE MODEL

A. First-principles calculations

The electronic structure of the system was determined using the full potential linearized augmented plane-wave method (FLAPW) [26] as implemented in the WIEN2K package [27]. In all the calculations the generalized gradient approximation (GGA) of density functional theory (DFT) was used with the exchange-correlation functional in the Perdew-Burke-Ernzerhof parametrization [28]. The integration over a 2D Brillouin zone was performed using the mesh densities corresponding to several hundreds of k points (or more) with the convergence criteria for energy, charge per atom, and forces set to 10^{-4} Ry, 10^{-3} e , and 1 mRy/a.u., respectively. The GaSe monolayers were separated by a distance of 14 Å ensuring the lack of hopping between the neighboring planes.

*weymann@amu.edu.pl

†maciej.zwierzycki@ifmpan.poznan.pl

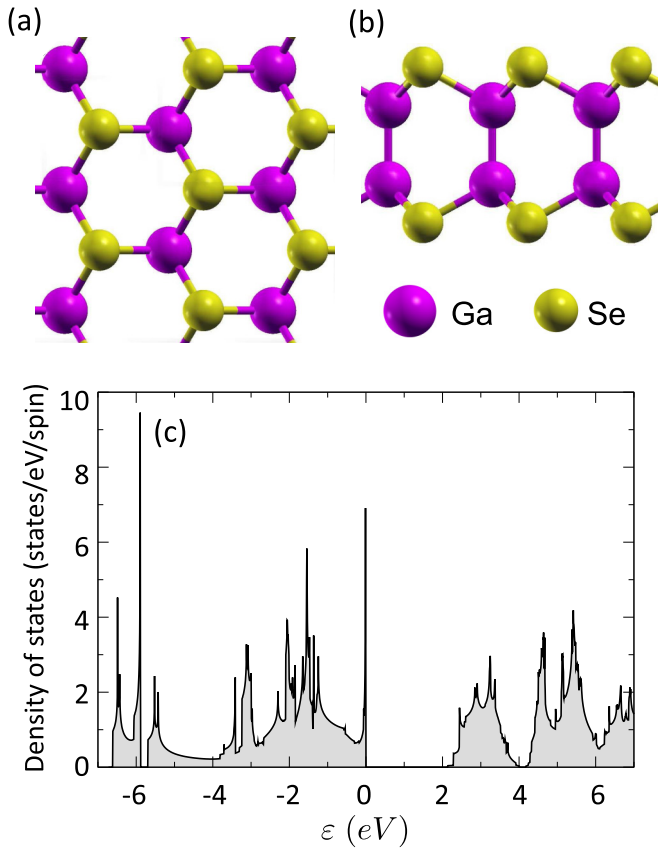


FIG. 1. The structure of the GaSe monolayer as seen (a) from the top and (b) from the side. (c) The density of states of unadorned GaSe monolayer.

The structure of the GaSe monolayer, consisting of two atomic layers, is shown in Figs. 1(a) and 1(b). In the first step, the lattice constant and the internal positions of four atoms within the unit cells were determined, the resulting parameters being $a = 3.755 \text{ \AA}$, $d_{\text{Ga-Ga}} = 2.46 \text{ \AA}$, and $d_{\text{Se-Se}} = 4.85 \text{ \AA}$ for the lattice constant and the distances between the Ga and Se atoms, respectively. The calculated values are in good agreement with the experimental data [29]. The density of states (DOS) calculated for an isolated monolayer is shown in Fig. 1(c). The value of the clearly observable band gap is equal to $\Delta = 2.1 \text{ eV}$.

A well-known deficiency of GGA, just as the basic local density approximation (LDA), is the systematic underestimation of the band gap. Our result is close to those reported in the literature for the same choice of exchange-correlation functional [7,9,23,29]. However, the calculations utilizing more advanced functionals [30,31] or the GW method [7,32], yield band gap values in the 2.7–3.0 eV and 3.4–3.9 eV range, respectively. A comparison of the band structures calculated using various methods (see, e.g., Ref. [30]) reveals them to be almost the same, but rigidly shifted. This is in particular true for the states near the band edges. However, for our further studies and the construction of an effective low-energy model the states around the Fermi energy are most relevant.

The experimentally reported values, obtained by either a scanning tunneling microscope (STM) [33] or optical

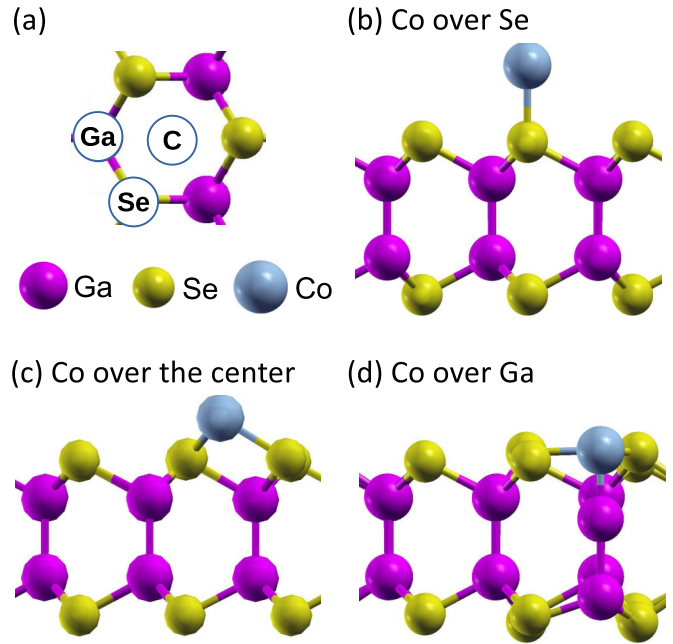


FIG. 2. (a) Three possible positions of the Co adatom—over Ga, Se, and over the center of the hexagon (marked as C)—as seen from the top. (b)–(d) Side views of the cases from (a) (relaxed structures).

spectroscopy [32,34] fall within the 3.1–3.9 eV range. We note that the demonstrated sensitivity of the band gap values to the thickness of the layer and to the strain [32] (imposed, e.g., by the substrate) can make the comparison between theory and experiment difficult. In spite of the differences in the calculated band gaps, the optimized lattice constants obtained using GGA, are typically within 1%–2% from the results of the more advanced approximations [31].

The case of a GaSe monolayer with a Co adatom was studied using a 3×3 supercell containing 37 atoms (18 Ga, 18 Se, and one Co atom). Within the supercell, the size of which was fixed to the multiple of the previously determined values, the internal positions were fully relaxed. The place for the most probable attachment of the adatom was determined by comparing the total energies for three high-symmetry cases with Co positioned over Se, Ga, and the center of the hexagon. These are indicated in Fig. 2(a), while the side views of the relaxed structures are shown in Figs. 2(b)–2(d). A visual analysis of the three structures suggests that the bonding strength is the weakest in the case of Co over Se [Fig. 2(b)] and the strongest for Co over Ga [Fig. 2(d)]. The Se-Co distance in the first case equals 2.46 \AA . In the second case of the centrally located adatom, its height over the plane of Se atoms is visibly smaller (1.27 \AA). On the other hand, in the third case, Co over Ga, the adatom is actually aligned with the Se plane.

The adsorption energies were calculated according to

$$E_{\text{ads}} = E_{\text{GaSe}} + E_{\text{Co}} - E_{\text{GaSe+Co}},$$

where E_{Co} and E_{GaSe} are the energies of the isolated Co atom and GaSe monolayer, respectively, so that positive values correspond to a binding case. The obtained values of -4.6 , -3.8 , and 2.7 eV , for “over Se,” “central,” and “over Ga,”

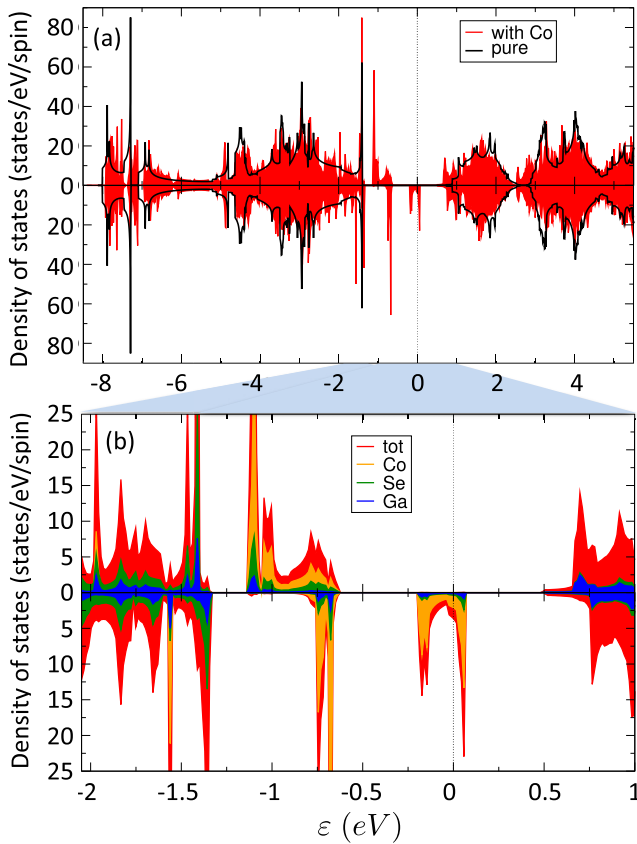


FIG. 3. (a) The density of states for GaSe with a Co adatom (red) together with the density of states of clean GaSe (black line). (b) The closeup of the behavior of the density of states around the Fermi energy, where the atomic contributions are also presented. The upper (lower) part of each panel presents the density of states for spin-up (spin-down). Note that the DOS of the pure GaSe layer does not show any magnetic order, i.e., the density of states is the same for both spin species.

respectively, indicate that the last configuration is not only lowest in energy but also the only binding one. The obtained value is close to the one found in Ref. [10] for the Fe adatom on the same substrate and falls in the general range of the adsorption energies reported for various adatoms on graphene [21,35] and graphenelike systems [36–38]. Both the adsorption energy value and structure displayed in Fig. 2(d) indicate the case of strong bonding.¹ The total magnetic moment, concentrated on the Co atom, ranges between atomiclike $3\mu_B$ for the “Co over Se” geometry, where Co is most distant from the GaSe layer, to the substantially reduced $1\mu_B$ in the lowest-energy case.

The density of states for the system with Co adatom, shown in Fig. 3(a) using the red color, follows for the most part an outline of the density of states for clean GaSe (black line). The most visible differences between the two densities are

¹The obtained value of E_{ads} is well above 0.6 eV, usually taken as the upper limit of the bond by the physisorption (weak bond via van der Waals forces) regime. This puts the system in the chemisorption (chemical bond, usually strong) range [39].

located in the energy window corresponding to the clean case gap.² This is shown in Fig. 3(b) where in addition to the total DOS (red), the atomic contributions are also shown. The latter are, in the case of Se (green) and Ga (blue), summed over all the atoms of the given kind within the supercell. The highly localized states visible within the region of the GaSe gap are of an almost pure Co- d character (predominantly $d_{x^2+y^2}$, d_{xy} , d_{xz} , and d_{yz}), although a certain level of hybridization with the surrounding atoms of the host can also be deduced.

In conclusion, the $1\mu_B$ value of the magnetic moment coupled with its almost complete localization on adatom suggests that the low-energy properties of the system under consideration can be correctly described using an effective spin- $\frac{1}{2}$ Anderson impurity model [40], as discussed in the following section.

B. Effective model

To obtain the most accurate results for the spectral properties of the Co adatom, we employ the density-matrix numerical renormalization group method [25,41], developed originally by Wilson for the Kondo problem [12]. The effective Anderson-like model for the NRG computations has been constructed following the method described in Refs. [22,42]. The crucial parameters of the Co adatom in this context are as follows: the on-site Coulomb repulsion (U), the level energy (ϵ), the hybridization parameter ($V_{pd\sigma}$), and the Co d -shell occupancy (n_d). The latter has been directly found from the *ab initio* calculations to be equal to $n_d = 7.6$. The parameter U for Co is equal to 4 eV [8], whereas the hybridization has been found to be $V_{pd\sigma} = -0.83$ eV by using the Harrison’s scaling method [43] for the computed distances $R_{\text{CoGa}} = 2.16$ Å (first-nearest neighbor) and $R_{\text{CoSe}} = 2.33$ Å (second-nearest neighbors). The charge states of the cobalt d level correspond to energies [42]

$$E(j) = j\epsilon + Uj(j-1)/2, \quad (1)$$

with the minimum value for $j_{\text{min}} \equiv n_d = 1/2 - \epsilon/U$, i.e., $\epsilon = -(n_d - 1/2)U$.³

The energy separations of the relevant levels $j = 7, 8, 9$ are $\tilde{\epsilon}_d = E(8) - E(7)$ and $2\tilde{\epsilon}_d + \tilde{U} = E(9) - E(7)$ and determine the parameters of the effective Anderson-like Hamiltonian, $H = H_{\text{Band}} + H_{\text{Hyb}} + H_{\text{Imp}}$. Here, H_{Band} is the Hamiltonian of electrons in the GaSe layer, H_{Hyb} describes the hybridization between the layer and Co adatom, while H_{Imp} models the adatom [22,42]. H_{Imp} is explicitly given by $H_{\text{Imp}} = \tilde{\epsilon}_d n + \tilde{U} n_{\uparrow} n_{\downarrow}$, where $n = n_{\uparrow} + n_{\downarrow}$ and n_{σ} is the occupation operator for an effective orbital level of the Co adatom for spin σ . For the energies of the effective Hamiltonian, one finds $\tilde{U} = U$ and $\tilde{\epsilon}_d = \epsilon + 7U = U(7.5 - n_d)$.

²One notes that the Fermi energy of the Co-decorated system is anchored within the region of the original gap because of the presence of the localized states discussed in the text.

³We compare the results of a mean-field limit of the Hubbard model with the results of the DFT calculations, thus putting both methods on a comparable level of approximation inasmuch as possible. As no further input is required from DFT results for a Co-adorned system, there is no need to introduce *double-counting* corrections, as is the case for LDA + U and similar approaches.

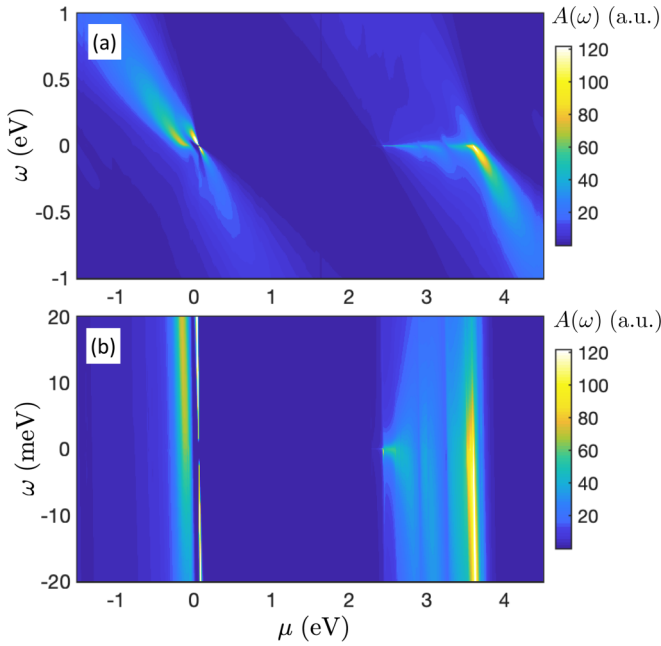


FIG. 4. (a) The zero-temperature spectral function of the Co adatom calculated as a function of chemical potential μ . (b) The low-energy behavior of the spectral function. The parameters of the effective Hamiltonian are $\tilde{U} = 4$ eV, $\tilde{\epsilon}_d = -0.4$ eV, and hybridization $V_{pd\sigma} = -0.83$ eV.

In calculations, we perform a logarithmic discretization of the density of states of pure GaSe. Then, we tridiagonalize the discretized Hamiltonian by the Lanczos method to obtain the hoppings and on-site energies along the Wilson chain [25]. In the next step, the eigenenergies and eigenvectors of the Hamiltonian are determined in an iterative fashion, which allows for the determination of the density matrix and the relevant spectral operators. To perform computations, we have assumed the discretization parameter equal to $\Lambda = 1.8$ and kept at least 1500 states at each iteration step. The quantity of interest is the spectral function $A(\omega)$ of the adatom, which is defined as $A(\omega) = -\text{Im}[G^R(\omega)]/\pi$, where $G^R(\omega)$ is the Fourier transform of the retarded Green's function of the adatom's effective orbital level.

At this point, it is important to note that the state-of-the-art methods employed in this paper allow us to generate reliable numerical results about the system transport properties. While the *ab initio* computations provide accurate information about the stable lowest-energy configuration of the system, NRG, known for its versatility and accuracy in solving the quantum impurity problems [44], enables an accurate solution of the effective low-energy model in the linear response regime. As a consequence, our results can be of importance in understanding or guiding future experiments on quasi-two-dimensional materials decorated with magnetic adatoms.

III. TRANSPORT PROPERTIES

The spectral function of the Co adatom $A(\omega)$ as a function of the chemical potential μ and energy ω is shown in Fig. 4(a), while the low-energy behavior of $A(\omega)$ is displayed in Fig. 4(b). The reference chemical potential $\mu = 0$

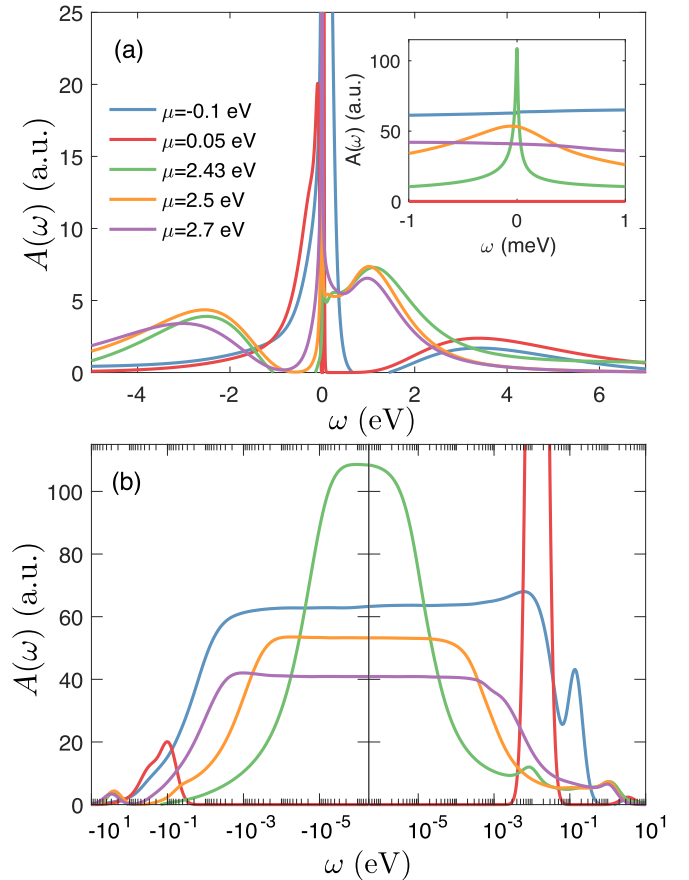


FIG. 5. The spectral function for selected values of the chemical potential μ plotted in the (a) linear and (b) logarithmic scale. The inset in (a) presents the low-energy behavior of the spectral function where a considerable Kondo peak is visible. The parameters are the same as in Fig. 4.

corresponds to the charge neutrality point of the studied system. We note that in experiments the chemical potential can be effectively controlled by a gate voltage. Because the density of states of pure GaSe exhibits a gap of the order of 2.1 eV [see Fig. 1(c)], the spectrum has a negligible weight at low energies in the corresponding regime of 0.2 eV $\lesssim \mu \lesssim 2.3$ eV. When the chemical potential is detuned out of this regime, the spectral function exhibits low-energy features resulting from strong correlations between the band electrons and the spin localized in the adatom's orbital. One such phenomenon is the Kondo effect, which manifests itself through a zero-energy resonance in the local density of states [11,12]. Indications of such resonances can be clearly seen in Figs. 4(a) and 4(b).

Moreover, the low-energy behavior of the Co adatom is also revealed in Fig. 5, which shows the energy dependence of $A(\omega)$ plotted both on the linear and logarithmic scale for selected values of the chemical potential. One can clearly identify the Hubbard resonances corresponding to $\omega + \mu \approx \tilde{\epsilon}_d$ and $\omega + \mu \approx \tilde{\epsilon}_d + \tilde{U}$. Interestingly, for all considered values of μ , except for $\mu = 0.05$ eV, there is a zero-energy resonance in the spectral function. This peak is clearly visible in the closeup on the low-energy behavior of $A(\omega)$ shown in Fig. 5(a) as well as in the logarithmic-scale dependence presented in Fig. 5(b). Because for the selected values of the

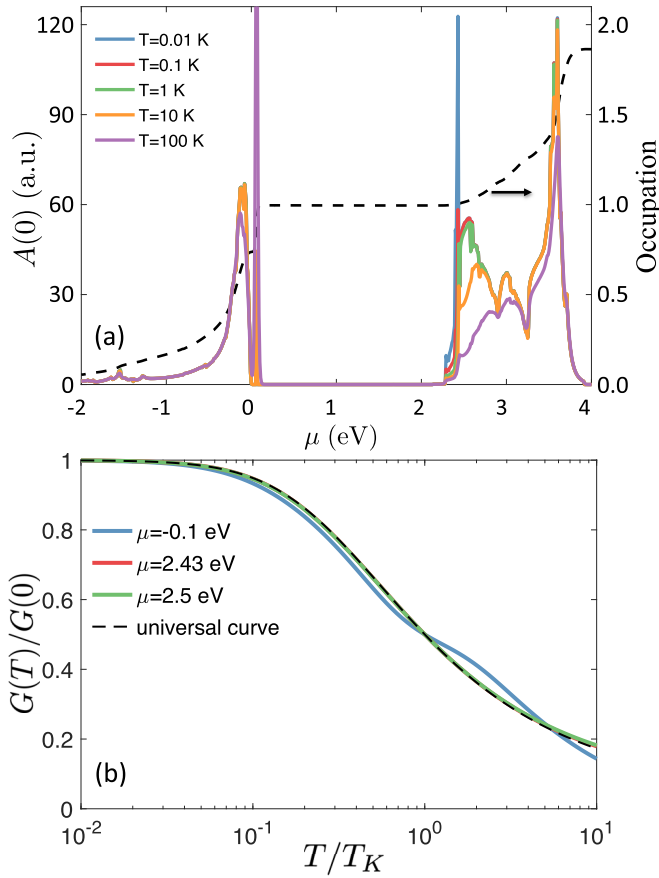


FIG. 6. (a) The spectral function at the Fermi energy $A(0)$ calculated for several values of temperature, as indicated. The dotted line presents the occupation of the adatom's orbital level. (b) The temperature dependence of the normalized linear conductance $G(T)/G(0)$ calculated for selected values of the chemical potential as a function of the normalized temperature T/T_K . The dashed line presents the universal scaling plot for the spin- $\frac{1}{2}$ Kondo effect. The parameters are the same as in Fig. 4.

chemical potential the adatom is mostly occupied by a single electron, one can conclude that the resonance is due to the Kondo effect. Here, however, one needs some care, since not all resonances need to be due to the Kondo correlations.

To shed more light on this issue, in Fig. 6(a) we present the chemical potential dependence of the spectral function taken at the Fermi energy $A(0)$. Because the Kondo resonance develops for temperatures T lower than the Kondo temperature T_K , $T \lesssim T_K$, a strong dependence of $A(0)$ on T can be observed for $\mu \lesssim 0.2$ eV and $\mu \gtrsim 2.3$ eV. Nevertheless, as mentioned before, special caution is needed since some low-energy features can be related to enhanced charge fluctuations around $\mu \approx \tilde{\epsilon}_d$ and $\mu \approx \tilde{\epsilon}_d + \tilde{U}$. More specifically, the effects associated with Kondo correlations develop only in the local moment regime [12], i.e., $\tilde{\epsilon}_d \lesssim \mu \lesssim \tilde{\epsilon}_d + \tilde{U}$, where the adatom's occupation is odd [see the dotted line in Fig. 6(a)]. To understand the origin of the low-energy resonances, we have determined the linear response conductance at different temperatures, which would correspond to, e.g., measuring the conductance over the Co adatom by an STM tip. The normalized conductance in the linear

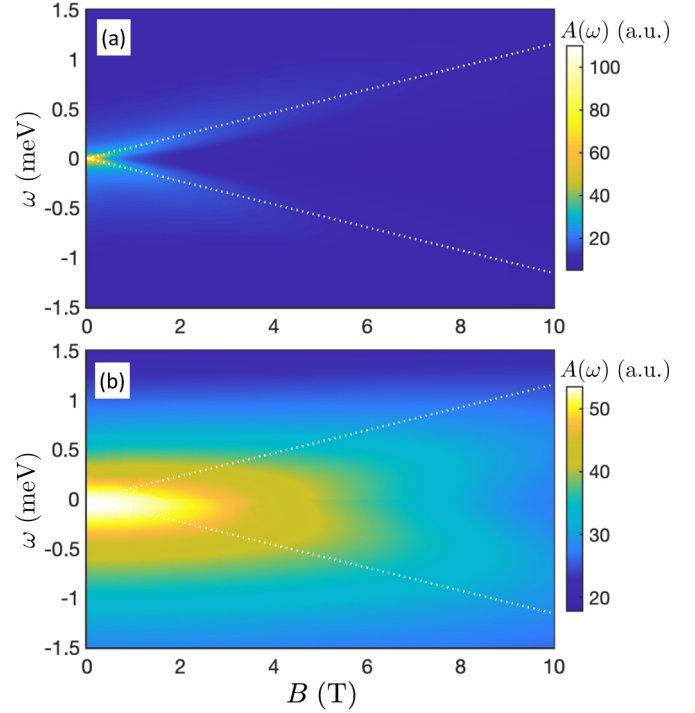


FIG. 7. Spectral function plotted vs magnetic field demonstrating the splitting of the Kondo resonance for (a) $\mu = 2.43$ eV and (b) $\mu = 2.5$ eV. The parameters are the same as in Fig. 4 and the g -factor was assumed to be $g = 2$. The dotted lines indicate the Zeeman splitting energy $\Delta_Z = g\mu_B B$. Note that in the case of $\mu = 2.5$ eV a larger magnetic field is necessary to suppress and split the Kondo resonance, which is associated with a larger Kondo temperature in this case compared to $\mu = 2.43$ eV.

response regime can be found from [45] $G(T)/G(0) = \int d\omega [-f'(\omega)]A(\omega)/A(0)$, where $f(\omega)$ denotes the Fermi-Dirac distribution function. In Fig. 6(b) we display the temperature dependence of $G(T)/G(0)$ as a function of the normalized temperature T/T_K , where T_K is the Kondo temperature defined as the temperature at which $G(T) = G(0)/2$. One can see that the resonances for $\mu = 2.43$ eV and $\mu = 2.5$ eV have the scaling characteristic of the Kondo effect— $G(T)/G(0)$ follows then exactly the universal scaling dependence of the spin- $\frac{1}{2}$ Kondo effect [12]. However, $G(T)/G(0)$ in the case of $\mu = -0.1$ eV does not match with the Kondo universal scaling and one can conclude that this resonance is not due to Kondo correlations, but rather associated with resonant charge fluctuations. We note that similar resonances have been observed in the case of silicene with Co adatoms [22].

Considering the Anderson model [12,40], such resonance develops when the occupation of the orbital changes as a function of level position and the energies of two neighboring charge states become degenerate. Its width is given by the strength of coupling to the host, which is typically much larger than the Kondo temperature, which determines the width of the Kondo peak. Moreover, this resonance does not show the characteristic spin splitting as in the case of the Kondo effect [12].

To corroborate our observations even more, in Fig. 7 we have determined the magnetic field dependence of the spectral

function for two selected values of the chemical potential, for which the temperature scaling of the conductance revealed the Kondo origin. Indeed, it can be clearly seen that the Kondo resonance becomes split by a magnetic field and only the side resonances at energies corresponding to the Zeeman energy $\omega \approx \pm \Delta_Z$ are present, where $\Delta_Z = g\mu_B B$ (see the dotted lines in Fig. 7). Note also that in the case of $\mu = 2.5$ eV a larger magnetic field is necessary to suppress and split the Kondo resonance, which is associated with the larger Kondo temperature in this case compared to $\mu = 2.43$ eV. This is why in the former case the splitting is less visible [see Fig. 7(b)] as compared to the case shown in Fig. 7(a).

IV. CONCLUSIONS

In this paper we have investigated the electronic and magnetic properties of the GaSe monolayer with a cobalt adatom. The focus has been put on the detailed analysis of the local densities of states, spectral functions, and the possible Kondo resonances and their evolution with an external magnetic field. The studies have been carried out in three steps by combining (i) the first-principles calculations, (ii) construction of an effective Anderson-type Hamiltonian, and (iii) the application of the numerical renormalization group. This allowed us to obtain very accurate and reliable predictions for the spectral properties of a Co-decorated quasi-two-dimensional GaSe layer.

In particular, the first-principles calculations provided the information about the lowest-energy configuration, the

magnetic moment, and occupation of the Co adatom. This information was further exploited to determine the parameters of the effective Hamiltonian and perform the NRG calculations. It turns out that the calculated local density of states of the Co adatom exhibits resonances depending on the position of the chemical potential. We have shown that these resonances can be associated with the Kondo correlations that develop between the adatom and two-dimensional host material. This observation has been corroborated by the analysis of the system's transport properties in an external magnetic field and finite temperatures. In particular, the splitting of the Kondo peak in the magnetic field as well as the Kondo universal scaling of the linear conductance have been demonstrated.

We believe that our study sheds new light on the spectral properties of magnetic adatom-decorated two-dimensional materials and, especially, on the Kondo phenomena in such systems. The results show that the Co-decorated GaSe monolayer is an attractive Kondo system and its properties can be tuned by gate voltage or an external magnetic field, which may be of importance for future electronics and spintronics applications.

ACKNOWLEDGMENTS

I.W. acknowledges support by the Polish National Science Centre from funds awarded through the decision No. 2017/27/B/ST3/00621. The computing time at the Poznań Supercomputing and Networking Center is also acknowledged.

-
- [1] A. Tiwari and M. Syväjärvi, *Advanced 2D Materials* (Wiley, Hoboken, NJ, 2016).
 - [2] X. Li and X. Wu, Two-dimensional monolayer designs for spintronics applications, *WIREs Comput. Mol. Sci.* **6**, 441 (2016).
 - [3] K. S. Novoselov, A. Mishchenko, A. Carvalho, and A. H. Castro Neto, 2D materials and van der Waals heterostructures, *Science* **353**, aac9439 (2016).
 - [4] P. Avouris, T. F. Heinz, and T. Low, *2D Materials: Properties and Devices* (Cambridge University Press, Cambridge, U.K., 2017).
 - [5] H. R. Jappor, Electronic structure of novel GaS/GaSe heterostructures based on GaS and GaSe monolayers, *Physica B* **524**, 109 (2017).
 - [6] H. R. Jappor and M. A. Habeeb, Optical properties of two-dimensional GaS and GaSe monolayers, *Physica E* **101**, 251 (2018).
 - [7] T. Cao, Z. Li, and S. G. Louie, Tunable Magnetism and Half-Metallicity in Hole-Doped Monolayer Gase, *Phys. Rev. Lett.* **114**, 236602 (2015).
 - [8] T. P. Kaloni, N. Singh, and U. Schwingenschlögl, Prediction of a quantum anomalous Hall state in Co-decorated silicene, *Phys. Rev. B* **89**, 035409 (2014).
 - [9] L. Ao, H. Y. Xiao, X. Xiang, S. Li, K. Z. Liu, H. Huang, and X. T. Zu, Functionalization of a GaSe monolayer by vacancy and chemical element doping, *Phys. Chem. Chem. Phys.* **17**, 10737 (2015).
 - [10] Y. Lu, C. Ke, M. Fu, W. Lin, C. Zhang, T. Chen, H. Li, J. Kang, Z. Wu, and Y. Wu, Magnetic modification of GaSe monolayer by absorption of single Fe atom, *RSC Adv.* **7**, 4285 (2017).
 - [11] J. Kondo, Resistance minimum in dilute magnetic alloys, *Prog. Theor. Phys* **32**, 37 (1964).
 - [12] A. C. Hewson, *The Kondo Problem to Heavy Fermions* (Cambridge University Press, Cambridge, UK, 1997).
 - [13] D. Goldhaber-Gordon, H. Shtrikman, D. Mahalu, D. Abusch-Magder, U. Meirav, and M. A. Kastner, The Kondo effect in a single-electron transistor, *Nature (London)* **391**, 156 (1998).
 - [14] G. Yoo, S.-S. B. Lee, and H.-S. Sim, Detecting Kondo Entanglement by Electron Conductance, *Phys. Rev. Lett.* **120**, 146801 (2018).
 - [15] S. Datta, I. Weymann, A. Płomińska, E. Flahaut, L. Marty, and W. Wernsdorfer, Detection of spin reversal via Kondo correlation in hybrid carbon nanotube quantum dots, *ACS Nano* **13**, 10029 (2019).
 - [16] I. V. Borzenets, J. Shim, J. C. H. Chen, A. Ludwig, A. D. Wieck, S. Tarucha, H.-S. Sim, and M. Yamamoto, Observation of the Kondo screening cloud, *Nature (London)* **579**, 210 (2020).
 - [17] T. O. Wehling, A. V. Balatsky, M. I. Katsnelson, A. I. Lichtenstein, and A. Rosch, Orbitally controlled Kondo effect of Co adatoms on graphene, *Phys. Rev. B* **81**, 115427 (2010).
 - [18] V. W. Brar, R. Decker, H.-M. Solowan, Y. Wang, L. Maserati, K. T. Chan, H. Lee, Ç. O. Girit, A. Zettl, S. G. Louie, M. L. Cohen, and M. F. Crommie, Gate-controlled ionization and screening of cobalt adatoms on a graphene surface, *Nat. Phys.* **7**, 43 (2010).

- [19] R. Chirla, C. P. Moca, and I. Weymann, Probing the Rashba effect via the induced magnetization around a Kondo impurity, *Phys. Rev. B* **87**, 245133 (2013).
- [20] J. Ren, H. Guo, J. Pan, Yu. Y. Zhang, X. Wu, H.-G. Luo, S. Du, S. T. Pantelides, and H.-J. Gao, Kondo effect of cobalt adatoms on a graphene monolayer controlled by substrate-induced ripples, *Nano Lett.* **14**, 4011 (2014).
- [21] D. Krychowski, J. Kaczkowski, and S. Lipinski, Kondo effect of a cobalt adatom on a zigzag graphene nanoribbon, *Phys. Rev. B* **89**, 035424 (2014).
- [22] I. Weymann, M. Zwierzycki, and S. Krompiewski, Spectral properties and the Kondo effect of cobalt adatoms on silicene, *Phys. Rev. B* **96**, 115452 (2017).
- [23] Y. Ma, Y. Dai, M. Guo, L. Yu, and B. Huang, Tunable electronic and dielectric behavior of gas and gase monolayers, *Phys. Chem. Chem. Phys.* **15**, 7098 (2013).
- [24] A. Rawat, R. Ahmed, Dimple, N. Jena, M. K. Mohanta, and A. De Sarkar, Solar energy harvesting in type II van der Waals heterostructures of semiconducting group III monochalcogenide monolayers, *J. Phys. Chem. C* **123**, 12666 (2019).
- [25] K. G. Wilson, The renormalization group: Critical phenomena and the Kondo problem, *Rev. Mod. Phys.* **47**, 773 (1975).
- [26] D. Singh, *Planewaves, Pseudopotentials, and the LAPW Method* (Springer, New York, 2006).
- [27] P. Blaha, K. Schwarz, G. Madsen, D. Kvasnicka, and J. Luitz, *WIEN2k, An Augmented Plane Wave + Local Orbitals Program for Calculating Crystal Properties*, edited by K. Schwarz (Technische Universität Wien, Austria, 2001).
- [28] J. P. Perdew, K. Burke, and M. Ernzerhof, Generalized Gradient Approximation Made Simple, *Phys. Rev. Lett.* **77**, 3865 (1996).
- [29] X. Li, M.-W. Lin, A. A. Puretzky, J. C. Idrobo, C. Ma, M. Chi, M. Yoon, C. M. Rouleau, I. I. Kravchenko, D. B. Geohegan, and K. Xiao, Controlled vapor phase growth of single crystalline, two-dimensional GaSe crystals with high photoresponse, *Sci. Rep.* **4**, 5497 (2014).
- [30] V. Zólyomi, N. D. Drummond, and V. I. Fal'ko, Band structure and optical transitions in atomic layers of hexagonal gallium chalcogenides, *Phys. Rev. B* **87**, 195403 (2013).
- [31] H. L. Zhuang and R. G. Hennig, Single-layer group-III monochalcogenide photocatalysts for water splitting, *Chem. Mater.* **25**, 3232 (2013).
- [32] D. V. Rybkovskiy, N. R. Arutyunyan, A. S. Orekhov, I. A. Gromchenko, I. V. Vorobiev, A. V. Osadchy, E. Yu. Salaev, T. K. Baykara, K. R. Allakhverdiev, and E. D. Obraztsova, Size-induced effects in gallium selenide electronic structure: The influence of interlayer interactions, *Phys. Rev. B* **84**, 085314 (2011).
- [33] Z. Ben Aziza, D. Pierucci, H. Henck, M. G. Silly, C. David, M. Yoon, F. Sirotti, K. Xiao, M. Eddrief, J.-C. Girard, and A. Ouerghi, Tunable quasiparticle band gap in few-layer GaSe/graphene van der Waals heterostructures, *Phys. Rev. B* **96**, 035407 (2017).
- [34] C. S. Jung, F. Shojaei, K. Park, J. Y. Oh, H. S. Im, D. M. Jang, J. Park, and H. S. Kang, Red-to-ultraviolet emission tuning of two-dimensional gallium sulfide/selenide, *ACS Nano* **9**, 9585 (2015).
- [35] X. Liu, C. Z. Wang, M. Hupalo, W. C. Lu, M. C. Tringides, Y. X. Yao, and K. M. Ho, Metals on graphene: Correlation between adatom adsorption behavior and growth morphology, *Phys. Chem. Chem. Phys.* **14**, 9157 (2012).
- [36] X. Lin and J. Ni, Much stronger binding of metal adatoms to silicene than to graphene: A first-principles study, *Phys. Rev. B* **86**, 075440 (2012).
- [37] H. D. Ozaydin, Y. Kadioglu, F. Ersan, O. Üzengi Aktürk, and E. Aktürk, Interaction of adatoms with two-dimensional metal monochalcogenides (GaS, GaSe), [arXiv:1711.10326](https://arxiv.org/abs/1711.10326).
- [38] H.-F. Lin, L.-M. Liu, and J. Zhao, Electronic and magnetic properties of transition metal decorated monolayer gas, *Physica E* **101**, 131 (2018).
- [39] D. Phil Woodruff, *Modern Techniques in Surface Science*, 3rd ed. (Cambridge University Press, Cambridge, U.K., 2016).
- [40] P. W. Anderson, Localized magnetic states in metals, *Phys. Rev.* **124**, 41 (1961).
- [41] Ö. Legeza, C.P. Moca, A.I. Tóth, I. Weymann, and G. Zaránd, Manual for the flexible DM-NRG code, [arXiv:0809.3143](https://arxiv.org/abs/0809.3143) (the open access Budapest code is available at <http://www.phy.bme.hu/~dmnrg/>).
- [42] O. Újsághy, J. Kroha, L. Szunyogh, and A. Zawadowski, Theory of the Fano Resonance in the STM Tunneling Density of States Due to a Single Kondo Impurity, *Phys. Rev. Lett.* **85**, 2557 (2000).
- [43] W. A. Harrison, *Electronic Structure and the Properties of Solids* (Dover, New York, 1980).
- [44] R. Bulla, T. A. Costi, and T. Pruschke, Numerical renormalization group method for quantum impurity systems, *Rev. Mod. Phys.* **80**, 395 (2008).
- [45] Y. Meir and N. S. Wingreen, Landauer Formula for the Current through an Interacting Electron Region, *Phys. Rev. Lett.* **68**, 2512 (1992).